Acta Cryst. (1962). **15**, 138

Simultaneous Diffraction: Indexing Umweganregung Peaks in Simple Cases

BY H. COLE, F. W. CHAMBERS AND H. M. DUNN

International Business Machines Corporation, Research Center, Yorktown Heights, New York, U.S.A.

(*Received* 9 *January* 1961 *and in revised form* 4 *April* 1961)

By simultaneous diffraction is meant those diffraction effects which occur when a single crystal is so oriented that more than one Bragg reflection is operative for a given monochromatic ray. These effects often are apparent on films and may seriously modify intensity measurements in Geiger counter diffractometry. The indexing of the planes involved in one class of these effects; namely, umweganregung, is worked out in some detail. Umweganregung peaks may be used as a precise measure of lattice parameter, as pointed out by Renninger.

Introduction

Simultaneous diffraction effects occur when a single crystal is so oriented in an X-ray beam that two, or more, sets of planes in the crystal simultaneously satisfy Bragg's law for a single wavelength. In terms of the reciprocal lattice, these effects occur when two, or more, lattice points lie on the Ewald sphere of reflection at the same moment. A particular selection of these effects can be observed when a single crystal is set in a diffractometer for a particular reflection, and then rotated slowly around the diffraction vector. When a second lattice point is brought onto the sphere of reflection by the crystal rotation, changes in intensity may be observed, especially if the first order reflection itself is very weak. Under these conditions, the simultaneous diffraction events often appear as peaks; they were first observed by Renninger (1937, 1955, 1960) at the 222 setting for diamond, and were described as 'umweganregung' or 'detour radiation' peaks by Ewald. In addition, in divergent-beam techniques, such as those reported by Lonsdale (1947) on 'extinction lines' and by Borrmann (1960) on 'anomalous transmission', the crossing of two or more lines on the photographs may be indicative of the excitation of these reflections at this point by a single ray in a common region of the crystal.

Most of the studies of simultaneous diffraction have used the umweganregung peaks observable at 'forbidden' reflection positions. Renninger used these 'Renninger Effect' peaks, as they are called, to obtain accurate lattice parameters for diamond; Warekois (1955) has looked into the possibility of using them to study perfection; and Fankuchen & Williamson (1956, 1959) have made perhaps the most complete study of the effect in an attempt to break the phase problem. Other investigations (James, 1954; Fraenkel, 1957; Cauchois *et al.*, 1937; Weigle *et al.*, 1937; Joynson, 1953) have also been reported.

With the growth of single crystal diffractometry, the availability of machine calculations, and the possibility of automation, it was felt that an awareness of these effects, and a review of indexing, might be of value.

Theory

Although graphical techniques are available for determining which sets of planes will contribute to 'umweg' peaks, the skill with which they must be drawn often taxes the patience if some accuracy is desired. It is, however, a straightforward procedure to write down the mathematical conditions that are satisfied when simultaneous diffraction exists, and with a little computation, machine computation if possible, to prepare charts to any desired precision for indexing in certain special cases.

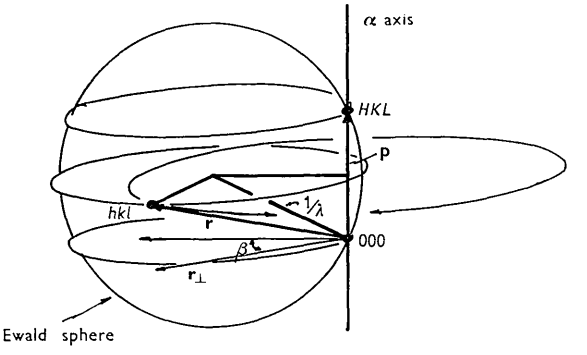

Fig. 1. Ewald sphere in reciprocal space at the moment when reflections are occurring from two lattice points, *HKL* and *hkl*. The vectors shown are defined in the text.

Fig. 1 represents the geometrical conditions existing in reciprocal space when the *hkl* reflection is on the Ewald sphere at the same moment as the *HKL* reflection. Let **P** and **r** be vectors to these two reciprocal lattice points. The radius of the sphere is $1/\lambda$, and the incoming beam may be represented by a vector $\mathbf{S}_0/\lambda = \mathbf{k}_0$. One sometimes adopts a 'sequential' point of view and thinks of the diffracted beam, $\mathbf{k}_0 + \mathbf{r}$, from the second set of planes, which we will call the operative reflection, as a new incident beam

inside the crystal. Since the vector from **r** to **P** is also a reciprocal lattice vector, defining what we will call the cooperative reflection, this new incident beam is diffracted by the cooperative planes into the primary, $\mathbf{k}_0+\mathbf{P}$, diffracted beam direction. Thus, as is well known, the indices of the cooperative reflection are obtained by subtracting the indices of the operative reflection from those of the primary reflection (James, 1954):

$$h'=H-h,\ k'=K-k,\ l'=L-l\,. \tag{1}$$

Obviously, since the above definitions of the beams can be interchanged, there must be a dynamical rather than sequential interaction between the beams. Some direct evidence of this is presented under 'surface effects' in a later section. The sequential idea is sometimes employed, however, in order to obtain approximate expressions for the intensities to be expected.

Returning to Fig. 1, choose **P** as an axis, and consider $\mathbf{k}_0$ and **r** in terms of their components along **P**, $\mathbf{k}_{0p}$ and $\mathbf{r}_p$, and in a plane perpendicular to **P**, $\mathbf{k}_{0\perp}$ and $\mathbf{r}_\perp$. With respect to $\mathbf{r}_\perp$ initially lying along $\mathbf{k}_{0\perp}$, the angle β between these vectors when **r** is brought onto the sphere represents the angle by which the crystal must be rotated about **P** to bring the reflection *hkl* into play. β is given by:

$$\cos\beta=\mathbf{r}_\perp.\mathbf{k}_{0\perp}/|r_\perp||k_{0\perp}|\,. \tag{2}$$

Since

$$\mathbf{r}_\perp=\mathbf{r}-\mathbf{r}_p=\mathbf{r}-(\mathbf{r}.\mathbf{P}/\mathbf{P}^2)\mathbf{P},$$

and

$$\mathbf{k}_{0\perp}=\mathbf{k}_0-\mathbf{k}_{0p}=\mathbf{k}_0+\mathbf{P}/2\,,$$

then

$$\cos\beta\,[(1/\lambda)^2-(P^2/4)]^{\frac{1}{2}}[r^2-r_p^2]=\mathbf{r}.\mathbf{k}_0-(\mathbf{r}.\mathbf{P}/P^2)\mathbf{P}.\mathbf{k}_0.$$

But

$$\mathbf{r}.\mathbf{k}_0=r^2/2;\ \mathbf{P}.\mathbf{k}_0=P^2/2; \tag{3}$$

therefore,

$$[(1/\lambda)^2-(P^2/4)]^{\frac{1}{2}}\cos\beta = \tfrac{1}{2}(r^2-r_pP)/[r^2-r_p^2]^{\frac{1}{2}}\equiv K_{hkl}^{HKL}\,, \tag{4}$$

where K_{hkl}^{HKL} is a constant for each pair of reflections considered. Equation (4) gives the necessary relationship between the two reflections and $\mathbf{k}_0$, for simultaneous diffraction to occur.

The constant K is a useful parameter. The denominator is always positive, but may be zero. In that case $K=\infty$ and **r** lies along **P** and no simultaneous diffraction is possible. The numerator may also be zero, or negative, which cases will be considered below; however, generally, K is a positive number.

For equation (4) to have a meaningful solution,

$$(1/\lambda)^2\geqq P_2/4\,, \tag{5}$$

which simply says that the Ewald sphere must be large enough for **P** to be on it. If K is positive, then there exists a longest λ (or smallest sphere) with both **P** and **r** on it, and with $\beta=0$:

$$(1/\lambda_m)^2-(P_2/4)=K^2. \tag{6}$$

As λ decreases, or the sphere gets larger, β increases steadily, until it reaches a maximum of 90° at $\lambda=0$. If K is negative, the crystal must be oriented with respect to the smallest sphere which contains **P** and **r** so that $\beta=180°$, and then β decreases to 90° as $\lambda\to 0$. For $K=0$, $\beta=90°$ for all λ, which implies that **r** lies on a circle of diameter P going through O and P. For a cubic system, equation (4) is conveniently handled in the form:

$$[(a/\lambda)^2-(P^2/4)]\cos^2\beta=K^2, \tag{7}$$

where (a) is the lattice parameter, and

$$P^2=H^2+K^2+L^2,\ r^2=h^2+k^2+l^2,\ \text{etc.}$$

In order to use equation (4) or (7) for indexing, these necessary conditions must be fitted into the geometry of a particular experiment. One of the simplest is the indexing of the Renninger peaks observed at the 'forbidden' 222 position in Ge. This experiment will be discussed in some detail in the following.

Renninger experiment

If, for example, a germanium crystal cut to expose a (111) face is mounted in a spectrometer, set so as to diffract Cu $K\alpha_1$ radiation from the 222 planes, and is then rotated around the diffraction vector, as shown schematically in Fig. 2, then the pattern shown in Fig. 3 is obtained. These 17 peaks are observed every 30° of rotation. We believe that this is the first time that the complete 'umweg' pattern at the 222 position in a diamond structure has been shown in full resolution. Due to the crystal symmetry, this pattern is reflected through the 30° mark, and then this larger 60° interval is repeated 6 times to make up the full 360° pattern. There are thus 204 peaks in the 360° of rotation. There would be even more peaks, except for the limitations imposed on certain *FCC* reflections by the diamond structure. The background between peaks is the true 222 reflection, plus contributions from diffuse scattering effects.

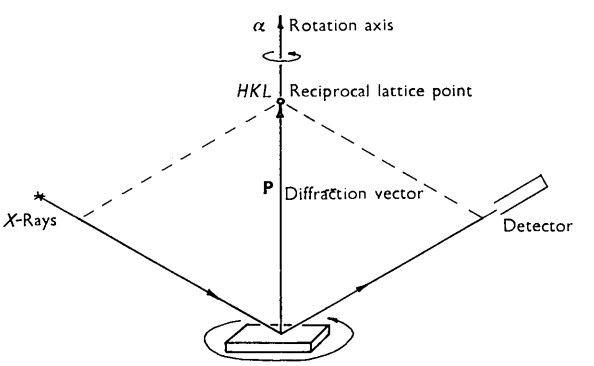

Fig. 2. Schematic representation of experimental arrangement used to obtain 'umweg' patterns. The crystal is rotated slowly around the diffraction vector.

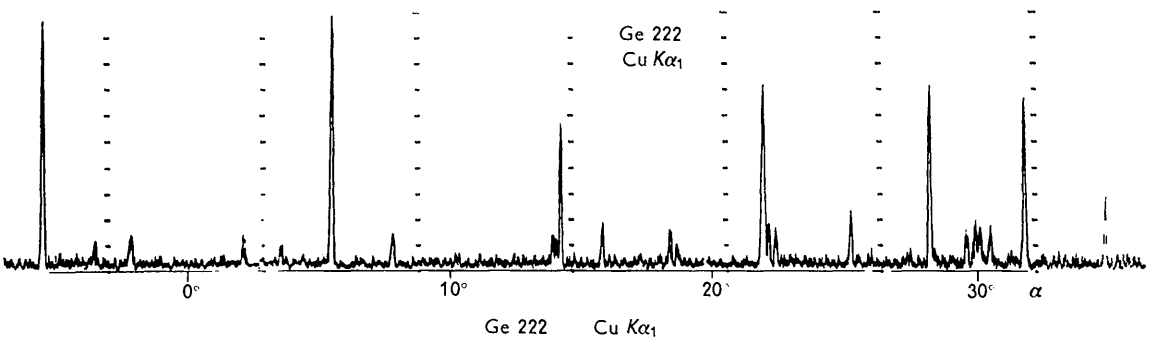

Fig. 3. 'Umweg' pattern at 222 position in germanium using Cu $K\alpha_1$ radiation. There are 17 peaks every 30° of rotation. The true 222 is part of the background level.

Even though Williamson & Fankuchen (1956, 1959) point out that their skew double-crystal monochromator improved the half-widths of the peaks, unmonochromatized but collimated radiation was used here. The collimation was such that the cross fire in any plane was less than the Cu $K\alpha_1$, α_2 separation for the 222 reflection. By this means, the power loss due to the presence of monochromators was avoided, while the divergence control permitted adequate angle and wavelength resolution. In order to optimize power further in later experiments a beam of 1 mm. × 1 mm. cross section was used with an evacuated pipe collimator 2 meters long to maintain divergence control. The counting rate at the peak of the strongest line is then approximately 600 counts/sec., and the $K\alpha_1$ or $K\alpha_2$ wavelength could be satisfactorily selected by changing the 2θ setting of the spectrometer. Also, without the monochromator in the system, $K\beta$, and Fe contamination radiation could also be used. The crystal was mounted on a Supper head in the *GE* single crystal orienter, and the alignment was adjusted until the strong peaks were of equal magnitude throughout the full 360° of rotation. The rotation around the diffraction vector was motor driven.

Indexing

The indexing of 'umweg' peaks is made simple by the fact that **P** is held on the sphere of reflection throughout the experiment. Also, since Ge is cubic, equation (7) may be used, in this case. There are often several reflections *hkl* which satisfy equations (4) or (7), for certain values of (a/λ), or for all values of (a/λ). Rather than search for these, an exhaustion procedure was used in the calculations, and all *hkl* were systematically investigated. If a plot of (a/λ) versus β is prepared, the curves for all combinations of **P** and **r** will be concave upwards, very roughly somewhat like parabolas. It is of little use, however, to plot all the curves centered on $\beta=0$; instead, an axis of reference, say **M**, is chosen perpendicular to **P**; and α_0, the angle between **M** and $\mathbf{r}_\perp$ is obtained from $\mathbf{M}\cdot\mathbf{r}$; then α, the angle by which this reference axis must be rotated from its zero position to bring **r** onto the sphere is given by:

$$\alpha=\alpha_0\pm\beta\,. \tag{8}$$

Fig. 4 is a plot of (a/λ) versus α for all the reflections operative in producing 'umweg' peaks at $P=222$ in a diamond structure. The scale of (a/λ) is inverted so that the curves appear concave downward. For each *hkl*, a curve of (a/λ) versus β is obtained from equation (7) and then this curve is centered at its proper α_0. A [110] axis was taken as reference axis, and $\alpha_0=0$ corresponds to this direction lying in the plane of $\mathbf{k}_0$ and **P**.

A chart such as shown in Fig. 4 would be used somewhat like a Hull chart. Since (a/λ) is known, at least approximately, a horizontal line drawn on the chart at this value predicts an 'umweg' peak at each angular setting where a curve is crossed. The index associated with the curve gives the 'operative' reflection, *hkl*.*

The chart can also be used to determine (a/λ) with some precision if an accurate 'umweg' pattern is given. For this purpose, the unit scale of Fig. 4 is too small. Fig. 5 is a section of Fig. 4 shown in larger scale, and is used as a working plot in the laboratory, since it covers the range of Fe to Cu radiation for Ge and Si.

A still larger scale is shown in Fig. 6, where the 'umweg' pattern is reproduced to demonstrate the indexing. As can be seen, the calculations predict 17 lines, all of which are clearly visible in the pattern. The horizontal dashed line is the calculated (a/λ) value for Ge and Cu $K\alpha_1$ radiation. The lower horizontal dash on the (a/λ) axis is the calculated value for Cu $K\alpha_2$. Just in going from α_1 to α_2 radiation by changing the 2θ of the diffractometer, quite a few changes in the pattern are observed to take place, and are discussed below.

* Ralph Moon, MIT, Lincoln Labs, has plotted $\varrho=[(a/\lambda)^2-p^2/4]^{1/2}$ versus α as a polar plot, a straight line resulting, as pointed out by O. Guentert. Plotted this way a given value of (a/λ) is a circle, and where it crosses the straight lines gives the indices. Private correspondence.

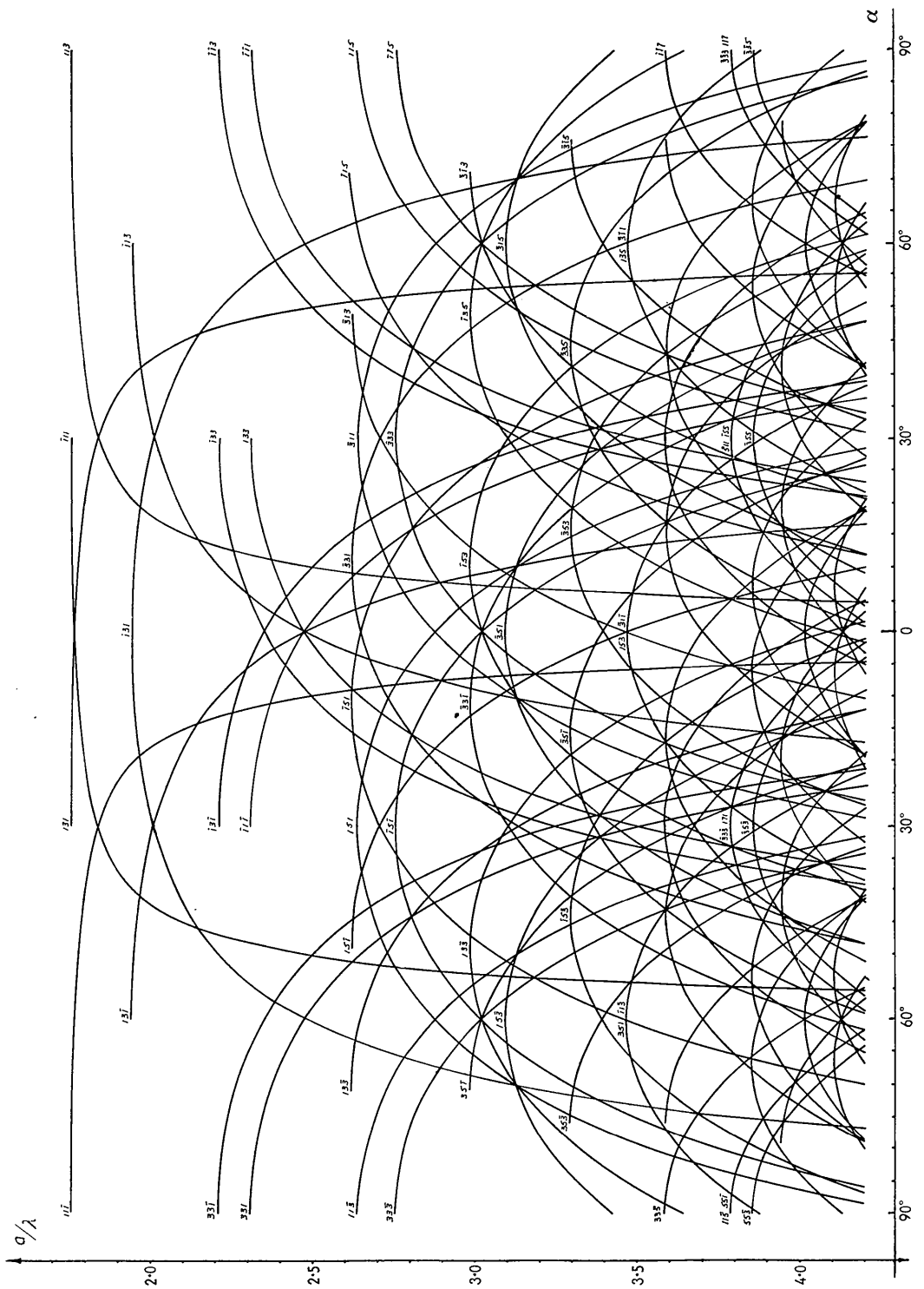

Fig. 4. Plot of (a/λ) versus α, the angle of rotation of the crystal about the diffraction vector, for the 'umweg' peaks at the 222 position in a crystal with a diamond structure. A horizontal line drawn at the proper value of (a/λ) predicts a peak at every curve intersection. The index of the 'operative' peak is read from the curve.

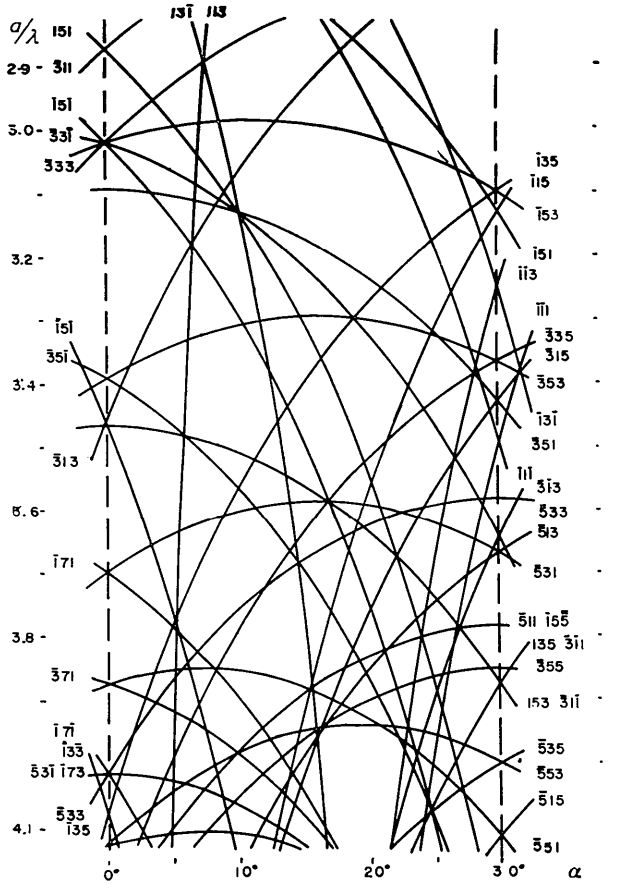

Fig. 5. A larger scale section of the plot shown in Fig. 4, useful for Fe and Cu radiation and germanium-like crystals.

Discussion of umweganregung pattern

In order to show something of the sensitivity available, certain of the peaks in Fig. 6 are shown in greater detail in Figs. 7, 8, and 9. Fig. 7 is the strongest line on the pattern. As can be seen from Fig. 5, the angular setting for this line scarcely changes with (a/λ), so that it makes a good reference line. Fig. 8 is the triplet of lines at $\alpha \approx 23°$, run with $K\alpha_1$ radiation (upper curves) and $K\alpha_2$ radiation (lower curves). The relative change of this small group with change in λ is easily seen. Fig. 9 is the very interesting group at $\alpha = 30°$. In going from $K\alpha_1$ (upper curves) to $K\alpha_2$ (lower curves), the center peaks cross over each other, and then cross over the outer peaks to become the new outer peaks in the $K\alpha_2$ run.

In Fig. 7, it is apparent that the background level,

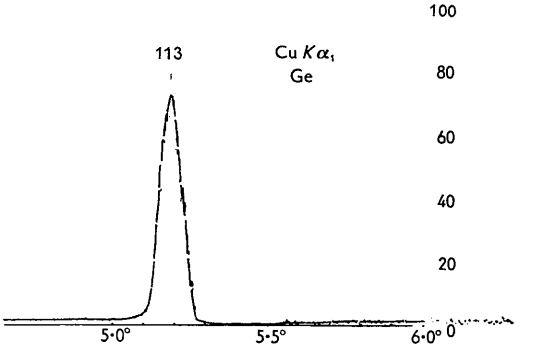

Fig. 7. The strongest line on the 'umweg' pattern for the 222 of Ge using Cu $K\alpha_1$ radiation. Note the suppression of the background on one side of the peak.

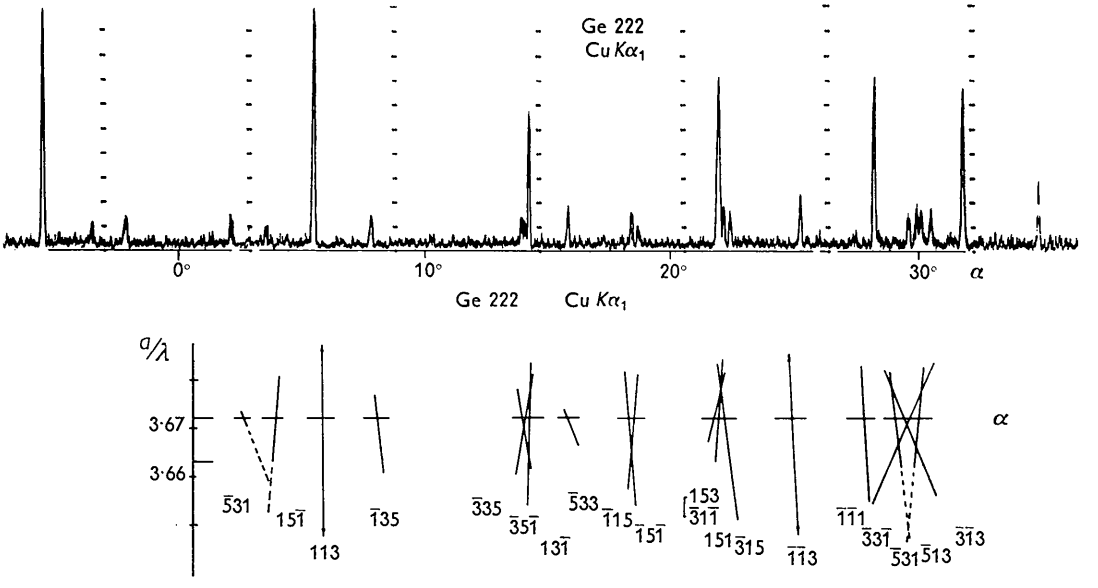

Fig. 6. A comparison of experimentally observed peaks and predicted peaks, given by the intersection of the dashed line and the curves. A change in λ from $K\alpha_1$ to $K\alpha_2$ would correspond to the lower dash, and several changes would be observed in the peak distribution. Had the dashed line gone through the curve intersection point at about 23°, five reflections would be on the Ewald sphere at once.

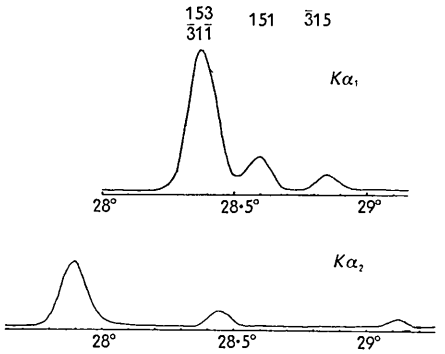

Fig. 8. The triplet of lines at $\alpha \approx 23°$ run with Cu $K\alpha_1$ (upper curves) and Cu $K\alpha_2$ (lower curves) radiations. The strongest line is a 'second order umweg' since for this peak three reflections are on the sphere. The angles shown are instrument readings.

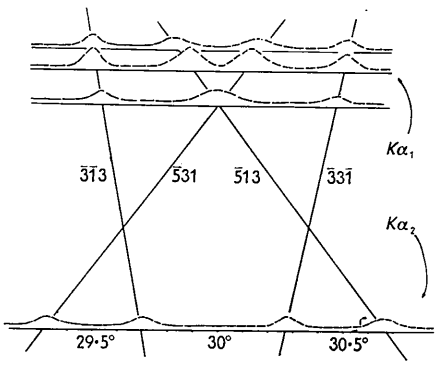

Fig. 9. The four peaks at $\alpha = 30°$. In going from Cu $K\alpha_1$ (upper curves) to Cu $K\alpha_2$ (lower curves) the inner peaks cross, then cross the outer peaks, and become the new outer peaks.

the 'true 222' plus 'background', is depressed on one side of the peak.

The strongest line of the triplet, Fig. 8, is a 'second order umweg' in the sense that three reflections are on the sphere. The particular pair, 153 and $\bar{3}1\bar{1}$ stay together for all λ. Other higher order effects occur only at special settings. For example, in Fig. 6, the triplet ($\alpha \cong 23°$) comes together in a single point for a slight increase in lattice parameter. At that setting, five points are on the Ewald sphere at the same moment. As can be seen from Fig. 4, the density of lines across the chart continues to rise as (a/λ) increases. Thus, as has been pointed out before (James, 1954), for electron diffraction, where $\lambda \sim 0{\cdot}05$ Å, the probability of simultaneous diffraction is very high.

Surface perfection

Referring to Fig. 1, if $\mathbf{r}_p$ is less than $\mathbf{P}/2$, the operative reflection is 'thrown into' the crystal. The cooperative reflection then throws the energy 'back out'. If $\mathbf{r}_p$ is greater than $\mathbf{P}/2$, then the operative reflection is initially 'thrown out' of the crystal, or 'along' the crystal surface, if $\mathbf{r}_p = \mathbf{P}/2$. Thus if simultaneous diffraction were sequential, relative changes in the 'umweg' pattern should occur if the surface were damaged. No evidence of a relative change was immediately apparent when a germanium (111) crystal surface was heavily ground, although in etching the surface damage away and running 'umweg' patterns between etchings, an optimum in the diffracted power was observed while surface damage was still apparent.

Lattice parameter

Although the measurement of lattice parameter by utilizing umweganregung peaks may be capable of great precision, the type of experiment described here offers no *increase* in precision over other normal techniques. In Fig. 8, for example, the change in angular separation of the outer peaks is approximately 0·75° for a change in λ of 0·0038 Å. We felt we could

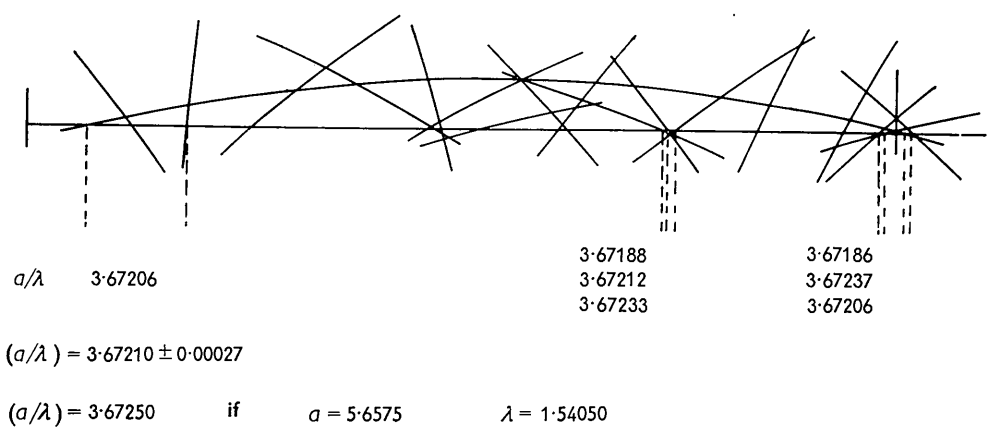

Fig. 10. A section of the (a/λ) versus α chart for Cu $K\alpha$ on Ge at the 222 position showing relative motion of the peaks for a change in (a/λ). (a/λ) was measured using the separations shown.

determine peak positions to 0·01°, therefore a change in separation of 0·02° may be detected, or a change in λ (or a) of about 0·0003 Å. This would be the order of the expected error in any series of measurements, just from resolution considerations. The crystal may be aligned as precisely as desired, since many peaks are available. Fig. 10 summarizes the values of (a/λ) obtained for this Ge crystal and Cu $K\alpha_1$ radiation, using the Renninger peaks shown in the figure (on the plot of (a/λ) versus α). We feel that the measured value of (a/λ) is significantly different from the accepted value, even if a refraction correction is applied; however, no attempt has been made to analyze the experiment any further than indicated here.

The authors would like to acknowledge the programming done by W. W. O'Neill to permit CRT output of the IBM 704 for tracing the curves.

References

BORRMANN, G. (1960). *Contributions to the Physics and Chemistry of the 20th Century.* Braunschweig: Vieweg.

CAUCHOIS, Y, HULUBEI, A. & WEIGLE, J. (1937). *Helv. Phys. Acta* **10**, 218.

FRAENKEL, B. S. (1957). *Bull. Res. Council Israel.* A, **6**, 125.

JAMES, R. W. (1954). *Optical Principles of the Diffraction of X-rays*, Chap. I. London: Bell.

JOYNSON, R. E. (1953). *MIT*, Ph. D. Thesis.

LONSDALE, K. (1947). *Phil. Trans.* A, **240**, 219.

RENNINGER, M. (1937). *Z. Phys.* **106**, 141.

RENNINGER, M. (1955). *Acta Cryst.* **8**, 606.

RENNINGER, M. (1960). *Z. Kristallogr.* **113**, 99.

WAREKOIS, E. P., Lincoln Labs Report Group 35, 37–41 (Aug. 1955).

WEIGLE, J. & MÜHSAM, H. (1937). *Helv. Phys. Acta*, **10**, 139.

WILLIAMSON, R. S. & FANKUCHEN, I., paper, Annual Meeting ACA, French Lick, Indiana, 1956, also RSI 30, 908 (1959).

Acta Cryst. (1962). **15**, 144

Crystalline forms of Bovine Pancreatic Ribonuclease. Some new Modifications

BY MURRAY VERNON KING*, JAKE BELLO†, EDITH H. PIGNATARO‡ AND DAVID HARKER§

Contribution No. 22 from the Protein Structure Project, Polytechnic Institute of Brooklyn, Brooklyn 1, *N.Y., U.S.A.*

(*Received* 15 *December* 1959 *and in revised form* 21 *February* 1961 *and* 5 *June* 1961)

Seven new crystalline forms of bovine pancreatic ribonuclease have been prepared and characterized by X-ray diffraction. One of these forms (XI) is obtained in the vicinity of the isoelectric point of the protein. Some are metal derivatives: VIII (Cu), X (Ni), XII (Hg). Two of the forms are obtained from aqueous methyl alcohol at different temperatures: IX and XIV. One of the forms (XII) is obtained from ribonuclease which had been treated with tribromoacetic anhydride.

Preparative techniques and materials

The techniques used in preparation of the seven new crystalline modifications of bovine pancreatic ribonuclease described here are all based on the methods outlined in a preceding paper (King, Magdoff, Adelman, and Harker, 1956; hereinafter denoted by KMAH). The letter designations applied in KMAH to the various methods of crystallization will be continued here also. The variations involve addition of metallic compounds, choise of solvent, pH control, protein-modification reactions, and temperature, and are described below in the sections devoted to the respective crystalline modifications.

* Present address: Orthopedic Research Laboratories, Massachusetts General Hospital, Boston 14, Mass.

† Present address: Dept. of Biophysics, Roswell Park Memorial Institute, 666 Elm St., Buffalo 3, N.Y.

‡ Present address: 230 Jay St., Brooklyn 1, N.Y.

§ Present address: Head, Dept. of Biophysics, Roswell Park Memorial Institute, 666 Elm St., Buffalo 3, N.Y.

The ribonuclease used in these studies was obtained from Armour Laboratories, lot numbers 381–059 and 647–213. (For convenience, ribonuclease may be abbreviated: RNase.) The solvents and reagents used were the purest commercially available, except that the solvent 2-methyl-2,4-pentanediol (abbreviated hereinafter as MPD) was further purified by adsorption of impurities on a cation-exchange column and distillation in vacuo from K_2HPO_4. When thus purified, MPD shows advantages over the simple alcohols as a medium for crystallizing RNase because of its lower tendency to induce alterations in the protein and its lower volatility.

Compositions of solutions are expressed below as volume percent of organic solvent in the final solution; it is understood that x volume percent of a solvent implies a mixture of x volumes solvent with $(100-x)$ volumes water. In samples prepared by method (*D*), addition of metal compounds and adjustment of pH are performed prior to freezing and addition of the